Parametric Optimization of Pulsed Nd:YAG Laser Lap Welding of Stainless Steel ASTM A240/ 316L with Carbon Steel ASTM A570/Gr30

Thaier A. Tawfiq

Institute of Laser for Postgraduate Studies
University of Baghdad /Iraq.

Abstract

This work describes seam welding process using dissimilar ferrous metals by pulsed Nd:YAG. The main objective of this work is to achieve the best welding conditions. This imposes careful selection for the welding parameters and inevitably the well design of experiment (DOE). Sheets of ASTM A240/316L stainless steel to ASTM A570/Gr30 carbon steel all of 0.5 mm in thickness were lap welded. Different pulse energies or the related peak power, pulse duration, pulse repetition rate, and welding speeds were used. Moreover, different welding speeds were controlled by the employed manipulator. The laser beam spot diameter and the standoff distance were fixed. Experimental results are supported by the computational 2D and 3D models. In this article response surface methodology (RSM) was applied to design the experiment and obtain the best parameters through a set of mathematical models that define the weld characteristics. The results show that the best joint in term of joint strength is obtained at 31.9 J pulse energy (related to 5.5 kW peak power and 5.8 ms pulse duration), power density of $1.43{\times}10^6$ W/cm^2, 1.5 Hz pulse repetition rate, and 0.5 mm/s welding speed.

Keywords: laser welding, stainless steel, low carbon steel, Optimization, RSM.

1. Introduction

Laser welding applications in various industries such as aerospace, automotive and shipbuilding are growing [1,2]. Initially CO_2 and recently Nd:YAG lasers have increased their role in welding processes due to their low distortion, precision, high production rate and process flexibility capabilities [2]. Presently, pulsed Nd:YAG become increasingly popular due to the efficient absorption of radiation by strongly reflective metals [3].

Heating metal sheet by a laser beam requires knowledge about the expected rise in temperature of the workpiece. The rise in temperature affects the weld bead geometry, weld velocity, gas flow rate, work piece hardness and microstructure [4]. The combination of the repetition rate and the possibility of shaping a pulse within significant pulse duration enable precise control of the heat supplied to the material [3]. The optimal set of parameters in pulsed Nd:YAG welding ensures

Excellent pulse to pulse stability, delivers the same preset energy, reduces the heat affected zone and increases reliability and repeatability Peak power density controls weld penetration.

Increasing the pulse width increases the weld dimensions and heat affected zone through increasing the heat conduction time. To increase weld width, reduce the thermal cycling and minimize depth variation, the pulse width is to be increased for introducing more conduction based welding mechanism [5,6]. The additional parameters are the pulse repetition rate and welding speed. A weld produced by a pulsed laser is composed of a number of overlapping spots.

The degree of overlapping of individual pulses expressed in percentage, i.e. the so-called overlap represents the degree at which the area of a material molten by a single pulse overlaps a similar area produced by the previous pulse. By means of a specific overlap the amount of heat supplied to a material being welded can be controlled, as well as the homogeneity of the weld structure [6]. Spot overlap percentage which is a function of speed, pulse repetition rate and focused spot diameter is used for determining the best laser for the job and for determining the total weld cycle time [6]. The sequential overlapped spots produce the joint zone which is characterized by the bead geometry, quality, hardness and microstructure.

These considerations depend on the spots overlapping percentage (*PER*) and duty cycle (*DC*). In addition to the combination of scanning speed (*v*), peak power (*P_P*), average power (*P_{av}*), pulse energy (*E_{pulse}*), pulse duration (*τ*), pulse repetition time (*PRT*), pulse repetition rate (*PRR*), laser off time (*OT*), intensity (*I*) and the spot size (*ω*). Equations 1, 2, and 3 describe this dependency [7,8]:

$$PER = 1 - \frac{v \cdot PRT}{2\omega + v \cdot \tau} \qquad \ldots (1)$$

$$DC = \frac{\tau}{PRT} \qquad \ldots (2)$$

$$PRT = \tau + OT \qquad \ldots (3)$$

The level of overlap determines the effective penetration. Good mechanical strength may be achieved at 40-60% overlap. However, for hermetic welding applications, 70-85% overlap is

typically required (Figure 1). As the welding speed is reduced the overlap is increased [6,7].
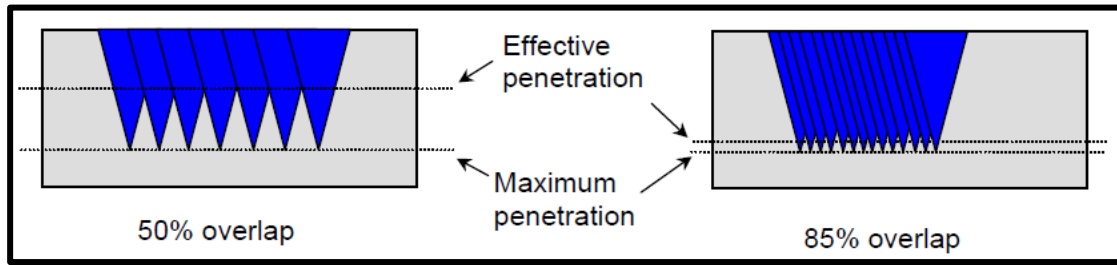
Figure 1: Schematic representation of overlap versus effective penetration depth for various overlap percentage [7].

The mathematical expressions associated with pulsed Nd:YAG laser material processing are defined as follows [9];

$$E = \tau \times P_P \qquad \dots (4)$$

$$E = \frac{P_{av}}{PRR} \qquad \dots (5)$$

$$PRR = PRT^{-1} \qquad \dots (6)$$

$$DC = \frac{P_{av}}{P_p} \qquad \dots (7)$$

According to the energy transfer mode and penetration depth there are two kinds of laser welding. The first is conduction welding, which is determined by the rate of intake of energy from the laser (intensity of the order 10^5 W/cm^2) and outtake of energy through the thickness of material by conduction. This leads to penetrate the weld by local melting without vaporization. The second is keyhole welding which occurs when the intensity exceeds 10^6 W/cm^2 that vaporizes a thin layer of the material. The vapor pressure pushes the molten aside forming a keyhole inside the weld pool along the depth filled with gas or plasma [10,11,12].

This work investigates the best working parameters that result the most successful weldments between stainless steel ASTM A240, Type 316L and ASTM A570/Gr30. This process is designed and optimized through DOE to reduce the experiment runs and to build an empirical model based on experimental results data for finding the optimum laser joining parameters. The DOE and the empirical model were carried out using Design Expert® package software Release 9.

2. Experimental Procedure
2.1 Materials

Both chosen metal sheets were joined by laser overlap welding process. The samples were prepared in dimensions of 100mm × 20mm × 0.5mm. Table 1 shows the chemical compositions (wt%) of these metals.

Table 1: The chemical composition of the welded metals.

Metal	C	Mn	Si	P	Cr	Ni	Mo	S	N	Cu	Fe
Stainless Steel ASTM A240, Type 316L	0.02	1.9	0.38	0.02	16.5	10.5	2.27	0.01	0.10	-	bal.
Carbon steel ASTM A570/Gr30	0.25	0.90	-	0.035	0.16	0.20	0.06	0.040	-	0.20	bal.

2.2 Experimental Arrangement

Both metals are placed in especially designed and fabricated clamps (Figure 2a) for ensuring 10 mm overlap configuration with a minimum air gap in between. In this setup the stainless steel sheets occupied the top side of the carbon steel sheets facing the laser source as illustrated in Figure 2b.
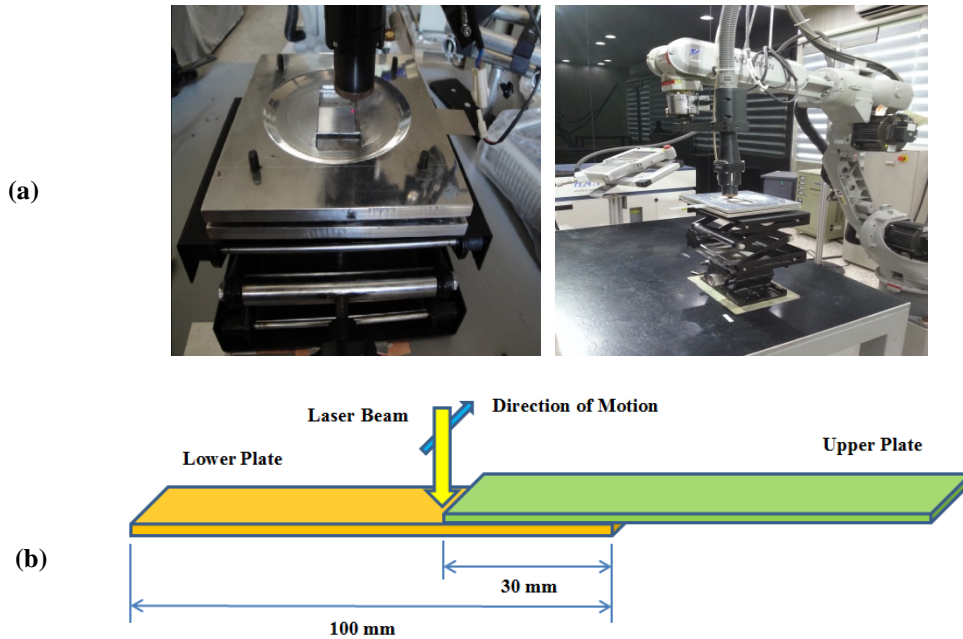
Figure 2: (a) clamps and (b) the lap joint configuration of the samples.

HAN'S LASER pulsed Nd:YAG laser apparatus of 1.064 μm wavelength, 8 kW peak power, up to 50 ms pulse duration, single pulse energy of 70/10 ms and up to 100 Hz pulse repetition rate was employed. The laser is delivered from the laser apparatus to the weld area via fiber optic of 400 μm in diameter through a focusing head that is installed on the robotic arm for ensuring steady and precise scanning speed and positioning. Figure 3 shows this experimental arrangement.

Figure 3: The employed experimental arrangement.

The laser spot of 0.7 mm in diameter was placed at the surface of stainless steel sheets. The standoff distance was 8 mm. Both metals share the spot in a configuration of half spot for each one as schematically presented in Figure 4. The welding process was executed for a single pass with the aim of argon gas to blow off plasma, prevent oxidation, and contribute cooling to the work piece.

The operating pulse shape was chosen to be of rectangular shape with 20% of the pulse duration for preheating and 20% for cooling process to ensure gradual heating and cooling during welding as illustrated in Figure 5.
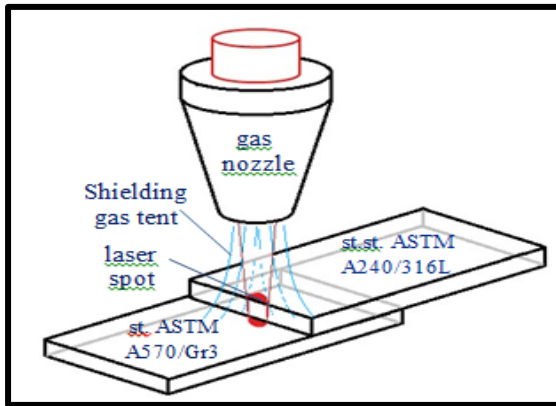
Figure 4: The welding setup**.**
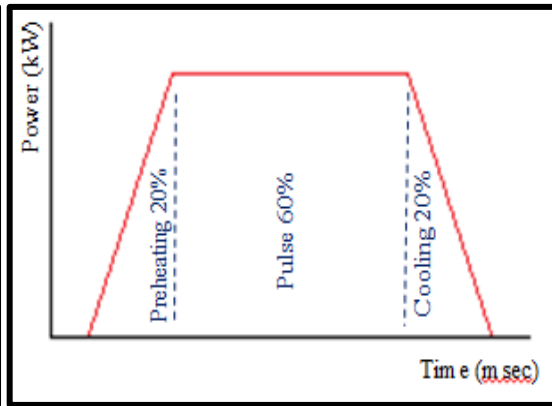
Figure 5: The operating pulse

3. Design of Experiment (DOE)

For investigating the experimental welding results and predicting the best conditions DOE based on response surface methodology (RSM) is used. RSM is a collection of mathematical and statistical techniques used for determining the optimum values of process response (output variable). Moreover, investigating the effect of process factors (input variables), which correspond to the response values and predicting the optimum experimental welding factors. The key welding factors are pulse energy (E), peak power (P_p), pulse duration (τ), pulse repetition rate (PRR) and scanning speed (*v*). RSM design is based on the central composite design (CCD) for creating a second order (quadratic) model for the response variables with no need to use a complete three-level factorial experiment. The second order model can be expressed by the following second-order polynomial relation [13]:

$$ y = \beta_0 + \sum_{i=1}^{k} \beta_i X_i + \sum_{i=1}^{k} \beta_{ii} X_{ii}^2 + \sum_{i=1}^{k-1} \sum_{j=2}^{k} \beta_{ij} X_i X_i + \varepsilon \qquad \ldots(9) $$

Where y is the response, *x* is the independent variables, *β* the regression coefficients and *ε* represents the error.

Table 2 shows welding parameters and RSM design levels which are used in this experiment. Using Design Expert V9 software package, the experiment processing trials were carried out with a series of runs wandering the space of input factors to identify the changes in response. Linear and second-order polynomials were fitted to the experimental data to obtain the regression equations. The sequential F-test, lack-of-fit test and complementary tests were computationally applied to generate the statistical and response plots and obtain the relevant model terms.

Table 2: The used independent factors and limits.

Factor	Unit	Code	Limits				
			-2	-1	0	+1	+2
P_p	kW	A	0.5	3	5.5	8	10.5
τ	Ms	B	2.5	4	5.5	7	8.5
v	mm/s	C	0.25	0.2	0.9	1.6	3.25
PRR	Hz	D	0.5	1	1.3	2.5	2.3

4. Results and Discussion

Experimentally, twenty samples divided into four groups each consists of five of them were carefully prepared to be lap welded. Preparation steps included cutting, making sharp edges and orthogonal, polishing and finally cleaning from dirt, oil and filings. All welded samples were subjected to shear strength test for measuring the breaking force of the weld zone. This test was held using a computerized tensile testing machine of the type (Universal Testing Machine/United/Tensile, Compression, Yield, Elongation / Germany) at "Specialized Institute for Engineering Industries (SIEI)". The entire experimental results are summarized in Table 3. It clarify that each group of samples underwent the process by varying one of the laser parameters and fixing the rest. Starting from group G1, the pulse energy (or peak power) of the best sample with the highest breaking force, working frequency and the scanning speed were fixed for all samples of group G2 while varying the pulse

duration. The same procedure was repeated for the rest groups. Finally, one of the twenty samples is chosen as the most successful one since it

Achieved the highest breaking strength out of all sample

Table 3: Classification of the tested samples and the working parameters.

Group No.	Sample No.	P_P (kW)	τ (ms)	E (J)	Irradiance W/cm^2	W. Freq (s^{-1})	Scanning Speed (mm/s)	Breaking Force (N)
G1	1	5.0	4.7	23.5	1.3×10^6	1.5	0.5	175
	2	5.5	4.7	25.85	1.43×10^6	1.5	0.5	367
	3	6.0	4.7	28.2	1.56×10^6	1.5	0.5	378
	4	6.5	4.7	30.55	1.69×10^6	1.5	0.5	411
	5	7.0	4.7	32.9	1.8×10^6	1.5	0.5	357
G2	1	5.5	4.5	24.75	1.43×10^6	1.5	0.5	352
	2	5.5	4.8	26.4	1.43×10^6	1.5	0.5	368
	3	5.5	5.2	28.6	1.43×10^6	1.5	0.5	382
	4	5.5	5.5	30.25	1.43×10^6	1.5	0.5	403
	5	5.5	5.8	31.9	1.43×10^6	1.5	0.5	489
G3	1	5.5	5.2	28.6	1.43×10^6	1.8	0.5	393
	2	5.5	5.2	28.6	1.43×10^6	2.0	0.5	398
	3	5.5	5.2	28.6	1.43×10^6	2.5	0.5	395
	4	5.5	5.2	28.6	1.43×10^6	2.8	0.5	391
	5	5.5	5.2	28.6	1.43×10^6	3.0	0.5	386
G4	1	5.5	5.2	28.6	1.43×10^6	2.8	0.3	346
	2	5.5	5.2	28.6	1.43×10^6	2.8	0.8	424
	3	5.5	5.2	28.6	1.43×10^6	2.8	1.0	431
	4	5.5	5.2	28.6	1.43×10^6	2.8	1.3	422
	5	5.5	5.2	28.6	1.43×10^6	2.8	1.5	416

Figure 6 shows the most successful four samples out of the whole groups.

Figure 6: Photo for the samples of the highest breaking forces per group.

A. Effect of pulse energy

In the first experiment variation of weld quality versus laser pulse energy or peak power (both are related) was investigated. Figure 7 illustrates the recorded breaking force for samples of G1 at different levels of pulse energy (A). By increasing the pulse energy (or peak power) the power density is increased up to the limit that causes the seam weld to be broad and deep enough to

achieve the higher breaking strength by evaporating a thin layer of the upper material causing a deep hole to be created inside the weld pool and reaching the lower sheet. This keyhole is an effective trap for the laser beam and will

significantly improve energy absorption from the laser beam. Increasing the power density more than this limit transfers the process from melting to vaporization leading to the weakening of the welding area.
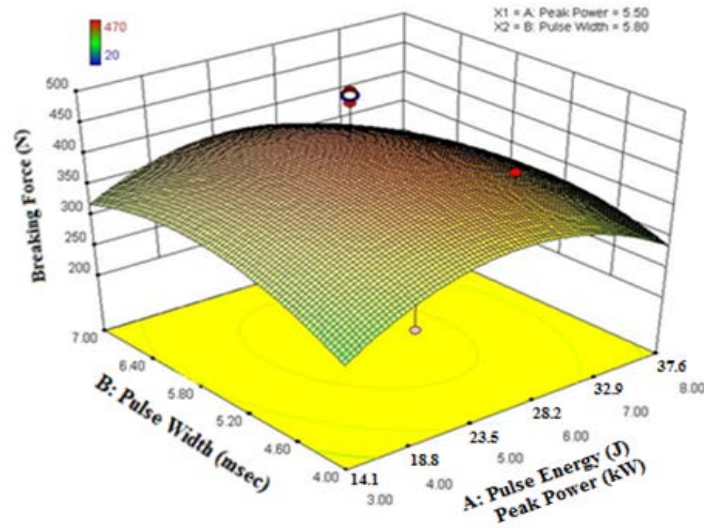
Figure 7: 3D representation for E or related P_P versus welding strength (X_1 for A/ E J and X_2 for τ ms).

B. Effect of pulse width

Figure 8 illustrates the recorded breaking force for samples of G2 at different levels of laser pulse width (B) as an investigation of weld quality due to this laser parameter at the same pulse energy (or peak power) that represents the most successful one for group1. The laser pulse energy is increased by increasing the pulse width at constant or with increased peak power (since E equals the product of P_P and τ)) leading to an increase in the rate of heat input into the material

which affects the process of melting and resulting a broader and deeper seam that achieves higher shear strength. For the seam weld processed by the same mean power, the variation in pulse duration eventually changes the resultant heating process dynamics. As such, the increase in pulse duration leads to somewhat faster operating speeds due to stronger heating effects. Increasing the pulse width beyond certain limit affects negatively the overlapping factor and resulting weaker seam welding.
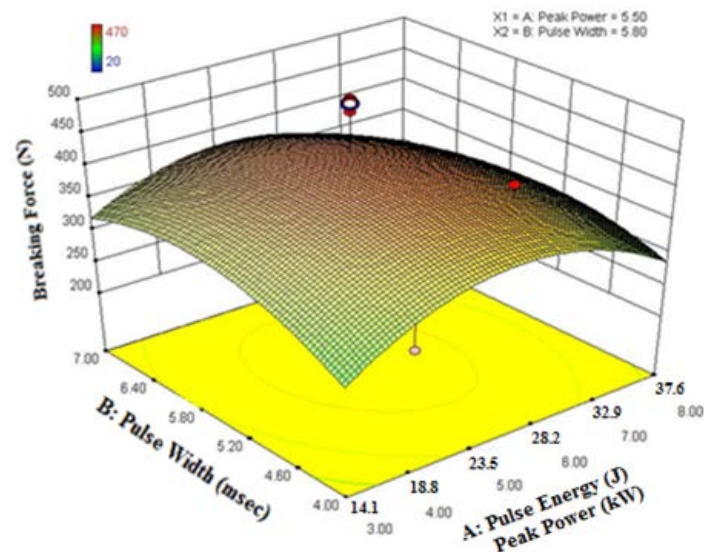
Figure 8: 3D representation for τ versus weld strength (X_1 for A/E J and X_2 for τ ms).

C. Effect of working pulse repetition rate

The third experiment investigates variation of weld quality versus working PRR. Figure 9 illustrates the recorded breaking force for samples of G3 at different levels of this parameter (C) using the best pulse energy and pulse width of

groups 1 and 2 respectively. Increasing PRR in the range under the maximum allowable limit (for the same E, τ and v) increases the overlapping per unit length resulting higher heat accumulation and producing better melting process with broader and deeper seam that achieves best breaking strength.
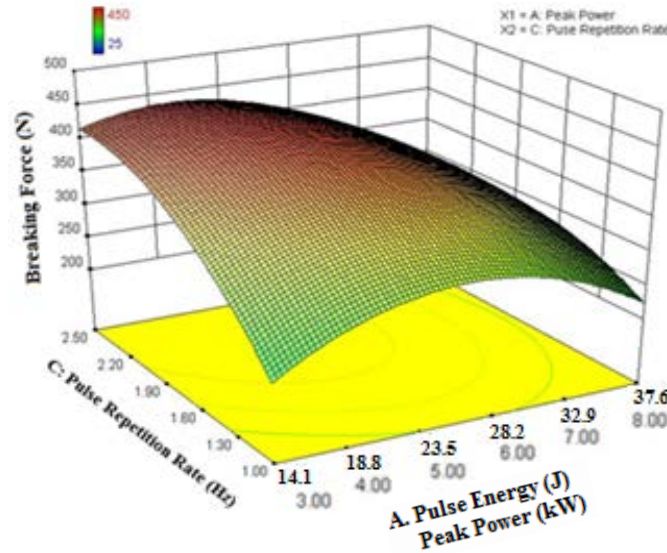
Figure 9: 3D representation for PRR versus weld strength (X_1 for A/E J and X_2 for PRR Hz).

D. Effect of welding speed

For investigating the effect of varying the welding speed on the weld quality, the fourth experiment is executed for samples of G4 at different levels of this parameter (C) using the best E, τ and PRR of groups 1, 2 and 3 respectively. Figure 10 illustrates the recorded breaking force for this case. At low speed the

overlapping is high enough to increase the chance of vaporizing the material directly under the laser spot due to the high generated heat accumulation resulting weak seam. Gradual increase the speed leads the overlapping factor to the limit that achieves the best breaking strength. Furthermore increase in the speed negatively affects the overlapping factor resulting narrower and shallower seam weld.
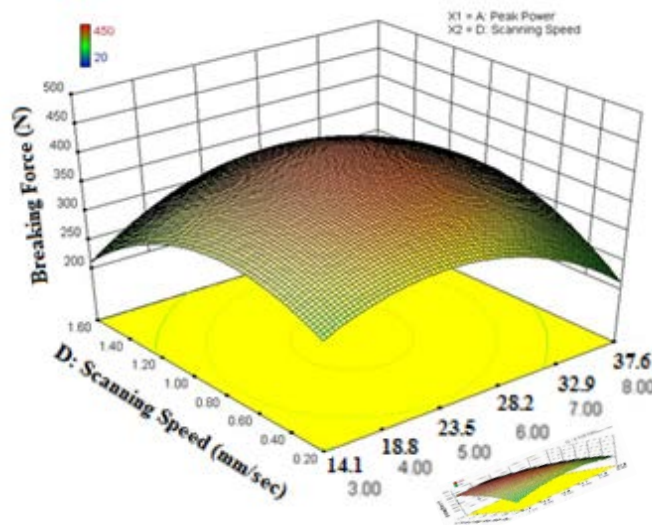
Figure 10: 3D representation for v versus welding strength (X_1 for A/E J and X_2 for v mm/s).

.

The apparent shape of the most successful samples that shows the highest breaking strength is shown in Figure 11.

G 1/4

G 2/5

G 3/2

G 4/3
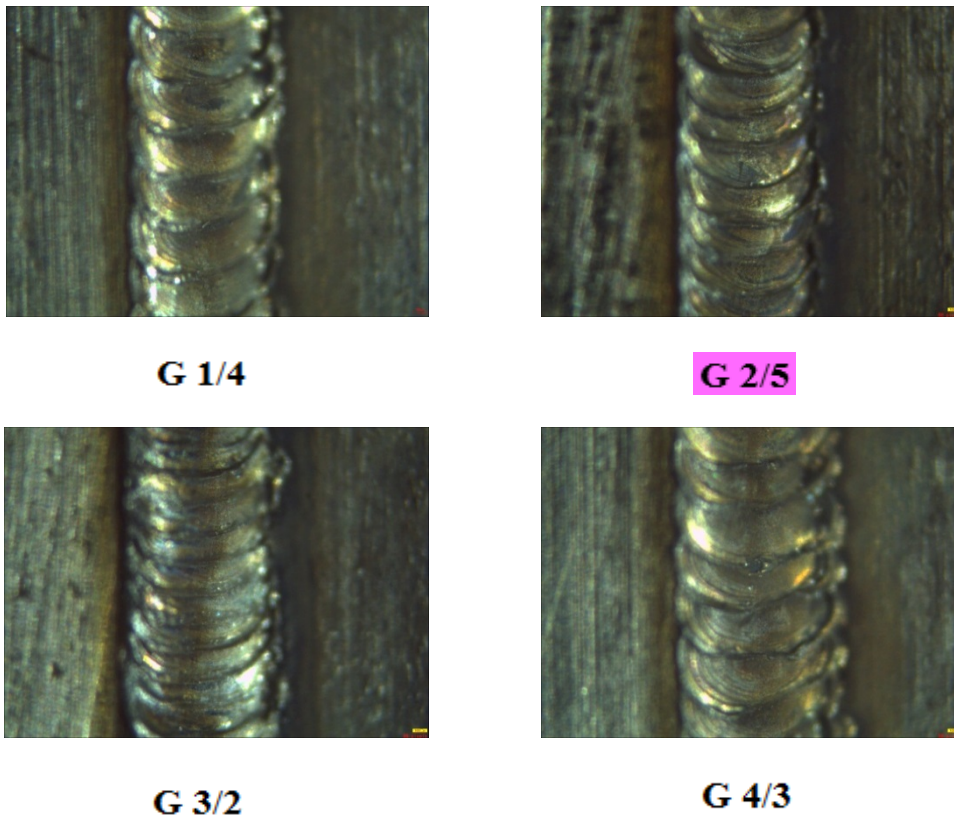
Figure 11: Apparent shape of the welding line for the best samples.

5. Conclusion

Lap welding of ASTM A240/316L stainless steel sheets to ASTM A570/Gr30 carbon steel sheets all of 0.5 mm in thickness by pulsed Nd:YAG without using filler material has been studied in this work. The experimental results show that;

➢ The operating working conditions that give good weld beads are controlled mainly by the pulse energy or the related peak power, pulse duration, pulse repetition rate and the travel speed.

➢ Rectangular pulses produce good quality welds in lap joints over the selected processing parameters.

➢ The quality of the process increases by increasing the pulse energy or the related peak power, pulse duration and the process speed up to certain limit. While a positive rising effect results by increasing the pulse repetition rate unless controlled by the other parameters.

➢ The best parameters that achieved best quality were 31.9 J of pulse energy (5.5 kW of peak power or irradiance of

1.43×10^6), 5.8 ms of pulse duration, 1.5 Hz of pulse repetition rate and 0.5 mm/s for the speed.

References

[1] Tzeng Y. F., Parametric analysis of the pulsed Nd:YAG laser seam welding process, 2000, Journal of Materials Processing Technology 102.

[2] M J Torkamany, M J Hamedi, F Malek and J Sabbaghzadeh, The effect of process parameters on keyhole welding with a 400W Nd:YAG pulsed laser, 2006, J. Phys. D: Appl. Phys. 39 (2006) 4563–4567.

[3] Jerzy Dworak, Impact of laser beam shape on YAG pulsed laser welding, 2012, Biuletyn Instytutu Spawalnictwa, Instytut Spawalnictwa, Welding Technologies Department.

[4] Tadamalle, A.P., Reddy, Y.P., Ramjee, E., Influence of laser welding process parameters on weld pool geometry and duty cycle, 2013, Advances in Production Engineering & Management, Volume 8, Number 1, pp 52–60.

[5] Ugur Caligulu, Mustafa Taskin, Haluk Kejanli, Ayhan Orhan, Interface characterization of CO_2 laser welded austenitic stainless steel

and low carbon steel couple, 2012, Industrial Lubrication and Tribology, Vol. 64 Iss 4 pp. 196 – 207.

[6] M.J. Torkamany, J. Sabbaghzadeh, M.J. Hamedi, Effect of laser welding mode on the microstructure and mechanical performance of dissimilar laser spot welds between low carbon and austenitic stainless steels, 2011, Materials and Design 34, 666–672.

[7] J. Sabbaghzadeh, M.J. Hamedi, F. Malek Ghaini, M.J. Torkamany, Effect of Process Parameters on the Melting Ratio in Overlap Pulsed Laser Welding, 2008, Metallurgical and Materials Transactions B, 340- Volume 39B.

[8] Y-F. Tzeng, Pulsed Nd:YAG Laser Seam Welding of Zinc-Coated Steel, 1999, Welding Research Supplement, Department of Mechanical Engineering, Chang Gung University, Taiwan.

[9] Arat Y, Dynamic behavior of laser welding plasma, 1986, Electron and Laser Beam Technology Development and Use in Material Processing, American Society for Materials, pp 397–406.

[10] Dumord E, Jouvard J and Grevey D, Modeling of deep penetration laser welding: Application to the CW Nd:YAG laser welding of X5Cr center dot Ni center dot 18-10, 1999, Laser Eng., 9, 1-21.

[11] H. Long, D. Gery, A. Carlier, P.G. Maropoulos, Prediction of welding distortion in butt joint of thin plates, 2009, Materials and Design 30, 4126–4135.

[12] A. Ruggiero, L.Tricarico, A.G.Olabi, K.Y.Benyounis, Weld-bead profile and costs optimization of the CO_2 dissimilar laser welding process of low carbon steel and austenitic steel AISI316, 2011, Optics & Laser Technology, 43, 82–90.